LEED intensity analysis of the clean W(100) c(2×2) surface reconstruction

1989 J. Phys.: Condens. Matter 1 1

(http://iopscience.iop.org/0953-8984/1/1/001)

J. Phys.: Condens. Matter 1 (1989) 1–12. Printed in the UK

LEED intensity analysis of the clean W(100) c(2 × 2) surface reconstruction

H Landskron, N Bickel, K Heinz, G Schmidtlein and K Müller
Lehrstuhl für Festkörperphysik, University of Erlangen–Nürnberg,
Erwin-Rommel-Strasse 1, D-8520 Elangen, Federal Republic of Germany

Received 20 June 1988

Abstract. A LEED structure analysis is performed for the W(100) c(2 × 2) surface reconstruction. Models with pure vertical displacements of the surface atoms can be clearly ruled out while others with predominant lateral displacements in the [11] and [01] directions result in a very good agreement with the experimental curves. However, a clear discrimination between these models is prevented by the insensitivity of normal incidence spectra to the direction of atomic displacements parallel to the surface. A minimum Pendry r-factor of $r = 0.26$ is achieved for a refined model suggested by Debe and King with a multilayer relaxation (first inter-layer spacing $d_{12} = 1.47$ Å, second inter-layer spacing $d_{23} = 1.60$ Å, and a reconstruction in the first and second layer with lateral displacements in the [11] direction (first layer: 0.24 Å; second layer: 0.02 Å).

1. Introduction

The reconstruction of the clean W(100) surface has been extensively investigated by LEED and other methods. With temperatures decreasing below 300 K, a reversible phase transition (Felter *et al* 1977, Yonehara and Schmidt 1971) from the unreconstructed (1 × 1) phase to the c(2 × 2) periodicity of the reconstructed phase takes place. As was shown by Wendelken and Wang (1985), the critical temperature depends on finite size effects such as surface conditions and domain sizes. Various models from different methods have been suggested for the reconstructed surface. For example, from FIM experiments (Tung *et al* 1982) and Debye temperature determinations (Heilmann *et al* 1979), the existence of vertical displacements in the reconstructed layer was concluded, while lateral displacements were extracted from LEED (Debe and King 1977, 1979) and helium scattering experiments (Stensgaard *et al* 1979). The LEED patterns in the experiments of Debe and King (1977, 1979) displayed a 2 mm point-group symmetry rather than the 4 mm symmetry of the substrate that is expected when all possible domains are equally developed. Therefore, Debe and King concluded, there is a predominance of one of the two domain orientations over the other, each of them having two-fold symmetry. Additionally, the $(\pm h/2, \pm h/2)$ and $(\pm h/2, \mp h/2)$ spectra turned out to be identical with regard to their relative intensities but different with regard to their absolute intensity level. This effect can be explained using a model with p2mg symmetry, which leads to systematic extinction of the $(\pm h/2, \pm h/2)$ beams of each

0953-8984/89/010001 + 12 $02.50

domain. The p2mg symmetry is only satisfied by a zig-zag structure with pure lateral displacements of the surface atoms in the [11] direction. Indeed, previous LEED calculations (Barker *et al* 1978, Walker *et al* 1981) yielded a better fit between theory and experiment for the zig-zag model (ZM) than for other c(2 × 2) reconstruction models. However, because of the enormous computational efforts required only a few structure models were tested with a very restricted set of geometry variations. Therefore, no definite decision in favour of a certain model could be made on the basis of these LEED calculations. However, with the development of powerful approximative computational schemes in recent years the test of different models extending over a large parameter space has become practicable. Therefore, new efforts have been made as reported in this paper in order to retrieve the correct structural model of the W(100) surface reconstruction. A new set of intensity data was measured for normal incidence, where the quality of the spectra was improved by the averaging of symmetrically equivalent beams. The measurements are described in the next section, while § 3 concentrates on the intensity calculations and the procedure that will result in the best fit between theory and experiment. Section 4 presents the results, which are summarised and discussed in § 5.

2. Experiments

The W(100) crystal was cleaned by several cycles of indirect heating at 1700 K in a 10^{-5} Pa oxygen atmosphere followed by a flash to 2200 K at 10^{-8} Pa. The latter corresponds to the residual gas pressure caused mainly by hydrogen. During the flash a pressure of 5×10^{-7} Pa was reached. The cooling of the sample was realised through contact with a reservoir of liquid nitrogen by means of copper laces, whereby a final temperature of 140 K could be reached about 20 min after the flash. However, the decrease in the residual gas pressure was much faster, i.e. a pressure of 1×10^{-8} Pa was reached within less than 5 min. So, at the intermediate temperature of 500 K, the pressure had already fallen to 3×10^{-8} Pa. Sharp superstructure spots appeared at 140 K; they began to weaken after about 20 min. This is assumed to be due to hydrogen adsorption from the residual gas, though no desorption measurements were performed. The intensity measurement was stopped 15 min after arrival at 140 K in order to avoid obtaining data affected by residual gas adsorption. Further measurement was triggered only by a new flash.

Intensity spectra at normal and oblique incidence of the primary beam were taken using a computer-controlled video camera facing a four grids LEED optics with the electron gun in the centre as usual. The technique allows the measurement of intensity–energy points for a single beam with a rate of 50 points s^{-1} providing simultaneous background correction (for details, see Heinz and Müller (1982), Heilmann *et al* (1985)). The normal incidence was adjusted by comparison of the spectra of symmetrically equivalent beams, whereby the quality of the data was finally improved by averaging. For normal incidence, nine symmetrically non-equivalent beams were measured. At off-normal incidence only an off-centre electron gun would allow measurements over a large energy range. As our electron gun is fixed at the screen's centre, a compromise between the angle of incidence and the accessible energy range had to be made. So, the data measured correspond to a polar angle of $\theta = 14°$ allowing the $(\frac{11}{22})$ beam to appear on the screen above 104 eV. The angle of incidence was checked by a numerical procedure described by Van Hove *et al* (1986).

3. Reconstruction models and intensity calculations

In contrast with the observations of Debe and King (1977, 1979), no asymmetry could be detected in the intensity of half-order spots in our measurements. The full 4mm symmetry is maintained through domain degeneracy and so no information from an individual domain can be extracted. Debe and King explain the observed 2mm symmetry in their experiment by the possible existence of steps causing the preferred orientation of domains. Indeed this effect could be demonstrated using an experiment by Wang and Lu (1982) applied to a high-density stepped surface with an average terrace width of 28 Å. The behaviour of the relative and absolute intensities of the half-order spots is fully compatible with the p2mg symmetry of the ZM suggested by Debe and King. These experimental facts as well as the results of previous LEED structure analyses (Barker *et al* 1978, Walker *et al* 1981) demand special attention in our analysis to the ZM (figure 1(*a*)), although the reconstruction geometry might be affected by the presence of steps and could be different from that of a step-free surface. Efforts are made to refine the ZM through the introduction of a multilayer relaxation and an additional zig-zag reconstruction in the second layer preserving the full p2mg symmetry (see the two-layer ZM in figure 1(*b*)). In order to check how slight deviations from the p2mg symmetry will modify the fit between theory and experiment, small vertical displacements in combination with the lateral zig-zag elongations are tried, as presented in figure 1(*c*), resulting in the so-called puckered zig-zag model (PZM). Furthermore, two completely different models are tested, the dimer model (DM) incorporating a dimer structure with lateral shifts of surface atoms in the [10] direction (figure 1(*d*)) and the 'vertical shift' model (VSM) involving pure up and down displacements parallel to the surface normal (figure 1(*e*)).

A CPU-time economic preselection of structure types without the need for time-consuming full dynamical calculations can be realised by the quasi-dynamical approximation (Heinz and Besold 1983, Bickel and Heinz 1985). This approximation scheme, which neglects intra-layer but preserves inter-layer scattering, is known to work reliably at higher energies and normal incidence. Therefore, a rough test of certain surface models is easily performed by the quasi-dynamical method, while the final refinement is left to a full dynamical structure determination. As the quasi-dynamical approximation can discriminate structures differing by vertical displacements of atoms with a sensitivity comparable to full dynamical calculations (Bickel and Heinz 1985), the approximation is applied to the VSM of figure 1(*e*) as well as to the ZM of figure 1(*a*), which is considered as a representative of the class of 'lateral shift' models (LSMs) (figure 1(*a*)–(*d*)). First, quasi-dynamical test calculations already performed for the ZM at normal incidence (Bickel *et al* 1987) exhibit an extreme insensitivity of the theoretical spectra to variations of lateral atomic displacements. Hence all refinement on the 'lateral shift' structure type (figure 1(*a*)–(*d*)) is done by full dynamical calculations (Pendry 1974, Van Hove and Tong 1979), which are carried out using the matrix inversion scheme for both the reconstructed surface and the bulk layers, while inter-layer scattering is treated by RFS.

The calculations exploit the high symmetry of normal incidence diffraction, which allows an optimum reduction in the number of beams to a minimum set of symmetrically inequivalent beams and saves considerable computer time. Here seven symmetrically inequivalent beams (10, 11, 20, 21, $\frac{11}{22}$, $\frac{13}{22}$, $\frac{33}{22}$) are exploited for the theoretical and experimental comparison in the case of the full dynamical calculations. Intensities are calculated in the energy range 20 eV to 251 eV in steps of 3 eV. Two additional beams,

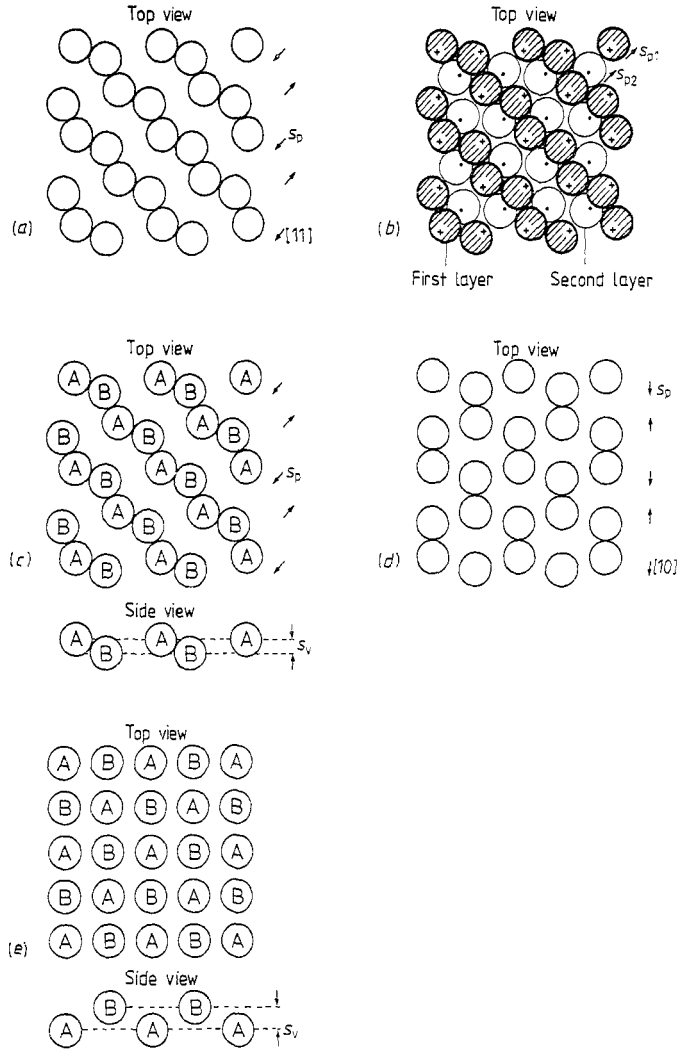

Figure 1. Surface structure models for W(100) c(2 × 2): (*a*) ZM with lateral displacements in the [11] direction; (*b*) two-layer ZM with a zig-zag reconstruction in the first and second layer; (*c*) PZM; (*d*) DM with lateral displacements in the [10] direction; (*e*) VSM.

namely the (22) and $(\frac{3}{2}\frac{5}{2})$ spot, are taken into account for the quasi-dynamical analysis, which extends from 101 eV to 351 eV where the approximation is known to work reliably (Heinz and Besold 1983). Up to ten (11) phase shifts are included in the full (quasi-) dynamical calculation. An inner potential of $(V_{or}, V_{oi}) = (-10\text{ eV}, -5\text{ eV})$ is chosen, where the adsorption is increased to $V_{oi} = -7$ eV for the quasi-dynamical approximation in order to achieve proper convergence. In the final *r*-factor analysis, V_{or} was allowed to shift by ±8 eV in steps of 1 eV giving a best fit for $V_{or} = -8$ eV. This value refers to the difference between the cathode and crystal Fermi levels and must be corrected by the corresponding difference in work functions. The resulting value is $V_{or} = -10.5$ eV. The phase shifts are corrected for thermal vibrations at $T = 140$ K using a Debye temperature of $\theta = 400$ K. In all cases the spacing from the first to the second layer d_{12} is varied from 1.39 to 1.61 Å (bulk value 1.58 Å) in increments of 0.02 Å, while lateral elongations s_p

of the ZM and DM are considered in the range 0.08 to 0.44 Å in steps of 0.04 Å. Vertical displacements s_v are incremented in steps of 0.08 Å for the VSM (figure 1(*e*)).

Additional calculations were performed for the ZM at off-normal incidence for a corresponding theoretical and experimental comparison at a polar angle of 14° and an azimuth of 146°. Enhanced computational effort caused by the loss of symmetry limited the energy range to a maximum value of 200 eV. The theoretical and experimental comparison includes spectra of nine integer- and six half-order beams. Lateral displacements s_p for both the ZM and DM were varied from 0.16 to 0.32 Å in steps of 0.04 Å.

4. Results

As mentioned in the previous section, a rough analysis is performed via the quasi-dynamical method to exclude clearly unfavourable models. Figure 2 compares the experimental and theoretical spectra of four beams, which result from quasi-dynamical calculations of the ZM and the VSM. The experimental curves are much better reproduced by the theoretical spectra of the ZM as compared with the spectra of the VSM, which display considerable discrepancies in comparison with the experiment for the half-order beams. A quantitative analysis using the Pendry *r*-factor (Pendry 1980) confirms the visual impression: a minimum *r*-factor of $r = 0.82$ for a distance from the first to the second layer $d_{12} = 1.41$ Å and a vertical elongation $s_v = 0.16$ Å indicate the misfit between theory and experiment in the case of the VSM. A lower *r*-factor of $r = 0.6$ expresses the improved fit between theory and experiment for the ZM at $d_{12} = 1.49$ Å and a lateral displacement of $s_p = 0.24$ Å. Although the value of $r = 0.6$ appears still rather high one has to keep in mind that an approximative method is used. Thus an *r*-factor of $r = 0.6$ can still extract the correct structure information when the quasi-dynamical approximation is applied to a reconstructed surface, as has been shown in previous work (Bickel and Heinz 1985). Therefore, the VSM can be rejected. Other reconstruction models with pure lateral displacements of the surface atoms not described in figure 1 produced *r*-factor levels very close to that of the ZM. Hence the quasi-dynamical method was found to be too rough for a discrimination between models of a lateral reconstruction type.

In order to achieve maximum sensitivity in lateral displacements, all further calculations on LSMs are performed using full dynamical calculations. Theoretical spectra of two half-order beams resulting from the ZM, PZM and DM are compared with the experimental curves in figure 3. The calculated spectra correspond to the same structural parameters $d_{12} = 1.47$ Å and $s_p = 0.24$ Å, which are close to the geometry of the best fit between theory and experiment achieved for each model. As demonstrated in figure 3 the $I(E)$-curves of the model calculations are very similar to each other. Considering the spectra of the ZM and DM with pure lateral displacements only, small differences in peak heights can be detected. All theoretical spectra reproduce the experimental curves quite well. The phenomenon of almost identical spectra from different LSMs is consistent with the results of previous work (Bickel *et al* 1987), where the theoretical $I(E)$-curves of the ZM did not change remarkably when the lateral displacement s_p was varied. Different LSMs were also tested by Walker *et al* (1981), whose results agree fully with our observations of an extreme insensitivity of the theoretical spectra to different lateral shift structures, although the authors (Walker *et al* 1981) had to operate with a very limited set of lateral shift variations s_p. The introduction of a small puckering of the zig-zag structure ((figure 1(*c*)) does not change the spectra noticeably, as can be seen in figure

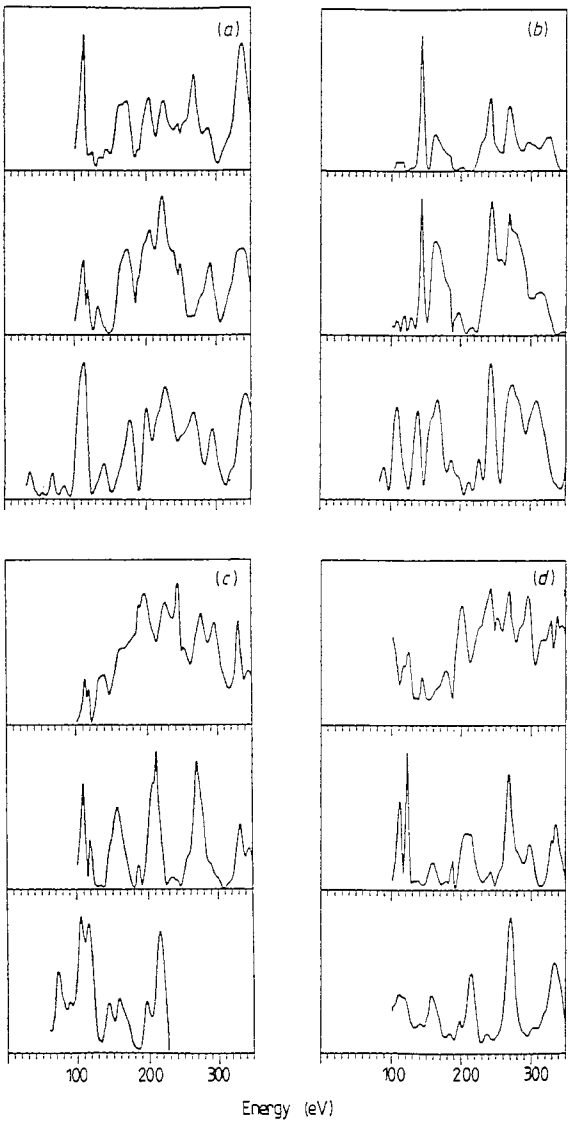

Figure 2. Quasi-dynamical calculated (best fit) spectra of (*a*) the (10), (*b*) the (11), (*c*) the $(\frac{11}{22})$ and (*d*) the $(\frac{13}{22})$ beams for (top) the VSM (figure 1(*e*)) and (middle) the ZM (figure 1(*a*)) in comparison with experiment (bottom); VSM: $s_v = 0.16$ Å, $d_{12} = 1.41$ Å; ZM: $s_p = 0.24$ Å, $d_{12} = 1.49$ Å.

3 when the puckering amplitude is restricted to 0.02 Å. Larger vertical displacements make the fit worse (see below).

The quantitative agreement between experiment and theory of different LSMs can be best visualised by *r*-factors. Figure 4(*a*) demonstrates the sensitivity of the Pendry *r*-factor with respect to the lateral shift s_p for the ZM. The *r*-factor minimum develops at a level of $r = 0.28$ (averaged over all beams) resulting in a best fit parameter of $s_p = 0.22$ Å with $d_{12} = 1.47$ Å. As already indicated by the visual inspection of the calculated $I(E)$-curves, the *r*-factor changes very slowly with variation of the s_p. The properties of the Pendry *r*-factor allow an easy determination of its variance Δr from which errors in the

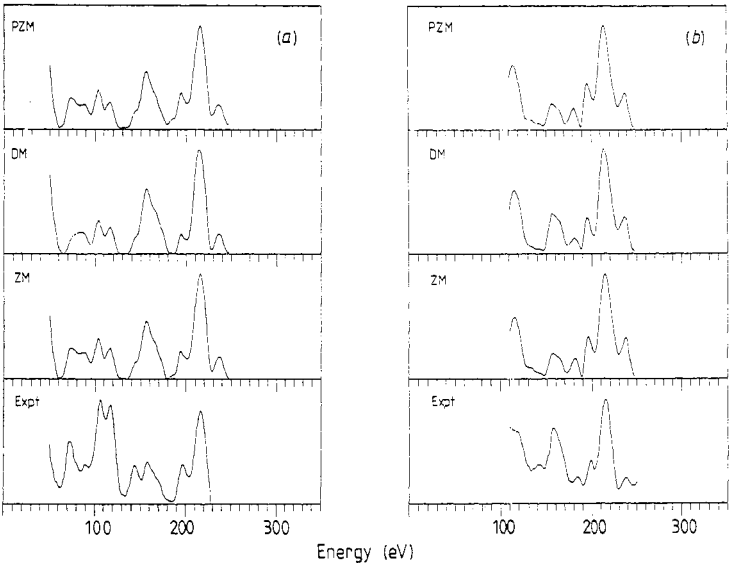

Figure 3. Experimental and theoretical (dynamical) spectra of (*a*) the $(\frac{11}{22})$ and (*b*) the $(\frac{13}{22})$ beam at $d_{12} = 1.47$ Å and $s_p = 0.24$ Å. The theoretical curves correspond to the ZM (figure 1(*a*)), DM (figure 1(*d*)) and PZM (figure 1(*c*), $s_v = 0.02$ Å).

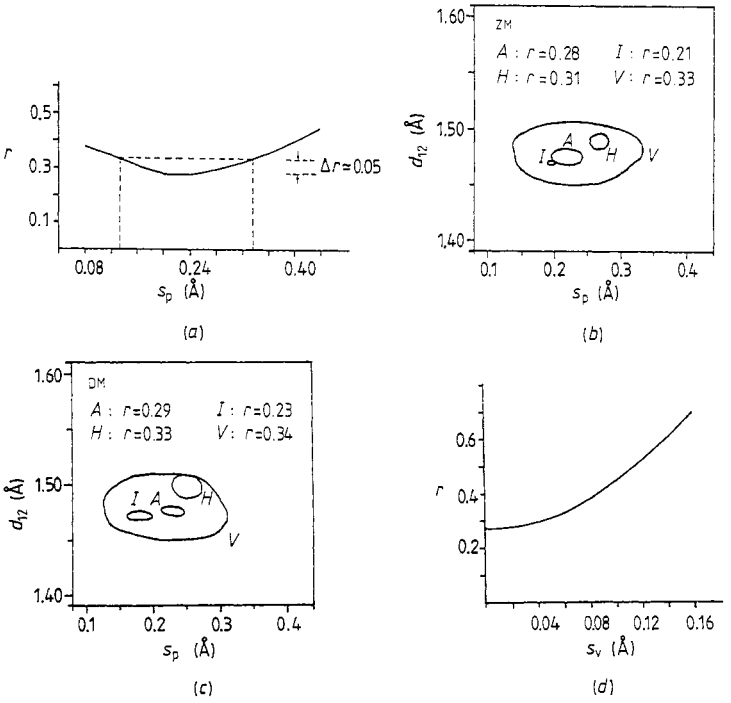

Figure 4. Pendry *r*-factors. (*a*) *r*-factor for the ZM (figure 1(*a*)) as a function of the lateral shift s_p at $d_{12} = 1.47$ Å. (*b*) and (*c*) contour maps with *r*-factors as a function of d_{12} and s_p for the ZM and DM: where I is the average over integer-order beams, *H* is the average over half-order beams, *A* is the average over the total of all beams and *V* is the variance 'sphere' for the average over all beams. (*d*) *r*-factor for the PZM as a function of s_v at $d_{12} = 1.47$ Å and $s_p = 0.24$ Å.

structural parameters can be estimated (Pendry 1980). In this example, the total common energy range of experimental and theoretical data amounts to $\Delta E = 1079$ eV resulting in a variance of $\Delta r = 0.05$. As shown in figure 4(*a*), an uncertainty $\Delta s_p = \pm 0.11$ Å in the lateral displacement follows from the variance Δr of the *r*-factor. Hence 'flat' *r*-factor minima lessen the significance of the structural results. This procedure is transferred into the two-dimensional parameter space of the contour maps for the ZM (figure 4(*b*)) and DM (figure 4(*c*)). In order to test the consistency of structural results obtained from subsets of data, *r*-factors are separately displayed as averaged over half-order, integer-order and all beams. A discrepancy between the *r*-factor minima of half- and integer-order beams shows up: the locations of the minima in parameter space do not coincide with each other. This can be stated for both the ZM and DM. The ZM exhibits its *r*-factor minima at $s_p = 0.27$ Å, $d_{12} = 1.49$ Å ($r = 0.31$) for the half-order and at $s_p = 0.19$ Å, $d_{12} = 1.47$ Å ($r = 0.21$) for the integer-order beams, whereas the *r*-factor minimum of the total of all beams appears at $s_p = 0.22$ Å, $d_{12} = 1.48$ Å ($r = 0.28$). As illustrated in figure 4(*b*) the scattering of 'subset data' results is stronger for the lateral displacement s_p than for the distance from the first to the second layer d_{12}. This is in line with the eccentricity of the 'contour ellipse' and holds also for the DM (figure 4(*c*)), for which the minimum *r*-factor, $r = 0.29$, for the total of all beams at $s_p = 0.23$ Å and $d_{12} = 1.48$ Å is comparable to the *r*-factor of the ZM. The *r*-factor minima of half- and integer-order beams lie within the variance 'sphere' (curves *V* in figure 4(*b*), (*c*)). For the ZM ($r = 0.28$), this gives error bars of about ± 0.11 Å for s_p and ± 0.03 Å for d_{12}. The comparably large error for s_p reflects the restricted sensitivity with respect to in-plane displacements, which prohibits a clear discrimination between the ZM and DM.

In order to test how a break in the exact p2mg symmetry will influence the structural results, the PZM (figure 1(*c*)) with additional vertical displacements is tested. A buckling of $s_v = 0.02$ Å at $d_{12} = 1.47$ Å and $s_p = 0.24$ Å does not change the *r*-factor ($r = 0.28$) of the 'pure' ZM (figure 1(*a*)). An increase in the buckling parameter s_v up to 0.04 Å leaves the *r*-factor level almost constant (see figure 4(*d*)), whereas a buckling of more than 0.06 Å increases the misfit between theory and experiment. Assuming a small buckling ($\leqslant 0.02$ Å) the intensity contribution to the spots of the exact p2mg symmetry might be within usual experimental error, so that the relative intensities of different $(h/2\ h/2)$ beams are not noticeably affected in the case of one domain being dominant over others. Hence a small deviation from the exact p2mg symmetry cannot be strictly excluded by the experimental observations.

The experimental facts (Debe and King 1977, 1979) favouring the ZM encouraged the authors to refine this model by introducing a second-layer relaxation and reconstruction (figure 1(*b*)). Of course all other models should be treated in the same way, however, the authors restricted the enhanced computational effort to the ZM, which is also favoured by a recent x-ray analysis (Robinson *et al* 1987). Assuming that atoms in the second layer will make way for zig-zag displacements (s_{p1}) of the atoms in the first layer the same reconstruction type seems likely for the second layer; however, with a smaller elongation amplitude (s_{p2}). Therefore, the corresponding zig-zag displacement s_{p2} was varied from 0.02 to 0.08 Å in steps of 0.02 Å. Theoretical and experimental spectra for the best fit are presented for all beams in figure 5. Figure 6 displays the *r*-factors as a function of the displacements s_{p1} and s_{p2} for the first and second layer, respectively, for $d_{12} = 1.47$ Å and $d_{23} = 1.58$ Å. The discrepancy between the *r*-factor minima of integer- and half-order beams exists still as well as the restricted sensitivity to variations of the s_{p1} and s_{p2}. The final adjustment to the structural parameters improves the *r*-factor, which becomes 0.26 giving $s_{p1} = (0.24 \pm 0.11)$ Å, $s_{p2} = (0.02 \pm 0.02)$ Å, $d_{12} = (1.47 \pm 0.03)$ Å and $d_{23} =$

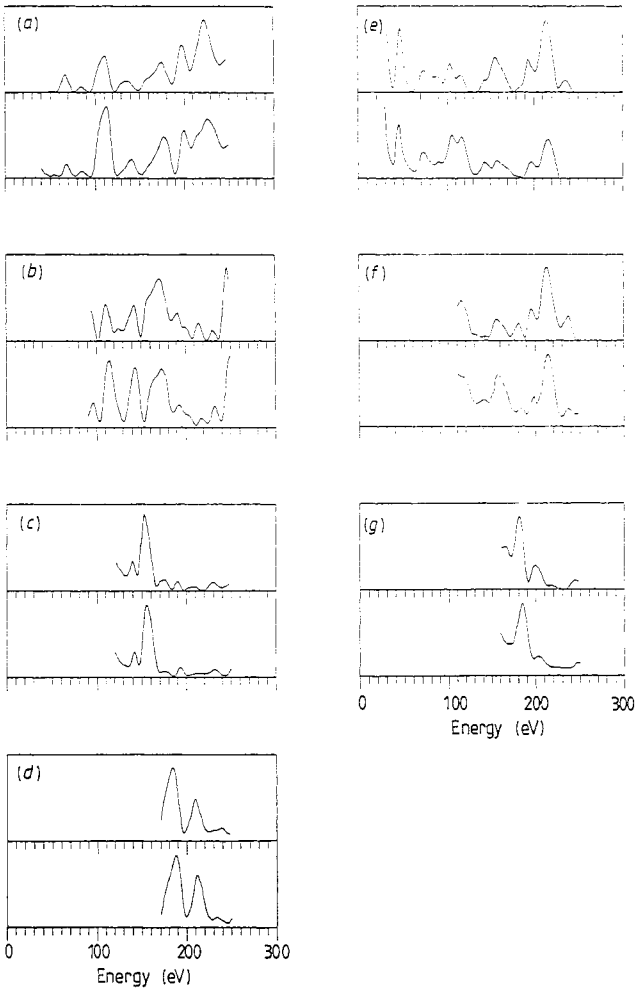

Figure 5. Experimental (lower) and calculated (dynamical) (upper) spectra of the two-layer ZM (figure 1(*b*)) for the best fit at $d_{12} = 1.47$ Å, $d_{23} = 1.60$ Å, $s_{p1} = 0.24$ Å and $s_{p2} = 0.02$ Å. (*a*) (10); (*b*) (11); (*c*) (20); (*d*) (21); (*e*) $(\frac{1}{2}\frac{1}{2})$; (*f*) $(\frac{1}{2}\frac{3}{2})$; (g) $(\frac{3}{2}\frac{3}{2})$ beam.

(1.60 ± 0.03) Å. These values agree rather well with the results of the recent x-ray structure analysis (Robinson *et al* 1987), where the zig-zag displacements were determined with $s_{p1} = 0.22$ Å and $s_{p2} = 0.044$ Å.

Temperature-dependent measurements of work functions and peak half-widths of half-order beams (Heilmann *et al* 1979) indicate that the phase transition from (1 × 1) to c(2 × 2) has not yet reached completion at $T = 140$ K. This may explain the discrepancy between the *r*-factors of half- and integer-order beams, as the intensities of integer-order beams could originate from a mixture of reconstructed and unreconstructed domains. If this is true, it is recommended that only the half-order beams be included in the structure analysis of the c(2 × 2) phase. However, this would not basically modify our structural results because of the restricted sensitivity to lateral displacements.

The latter restriction may be overcome by data analysis of the oblique incidence of the primary beam. This was tried for the ZM at a polar angle of 14° and an azimuth of 146°, values which result from the restrictions explained in § 2. Figure 7 presents the

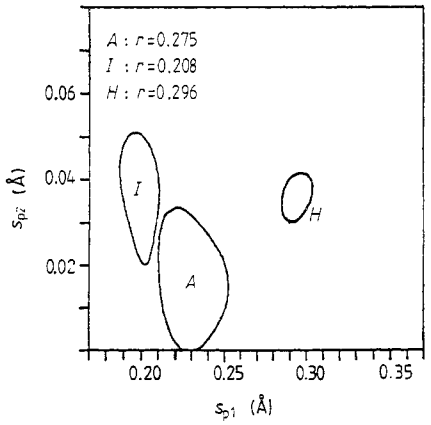

Figure 6. *r*-factors of the two-layer ZM (figure 1(*b*)) as a function of s_{p1} and s_{p2} at $d_{12} = 1.47$ Å (for I, A), $d_{12} = 1.49$ Å (for H) and $d_{23} = 1.58$ Å, where I is the average over integer-order beams, H is the average over half-order beams and A is the average over the total of all beams.

corresponding *r*-factors as a function of s_p and d_{12}. Clearly the sensitivity to s_p did not improve as compared with the case of normal incidence. This can be explained by the choice of a too small polar angle and by an average taken over all beams. This destroys a possibly higher sensitivity of a single beam which was observed for the $(\frac{11}{22})$ spot by theoretical tests. Therefore, only a sensitive subgroup of beams should be chosen for the fit. However, this could not be realised in our case because the energy range of the

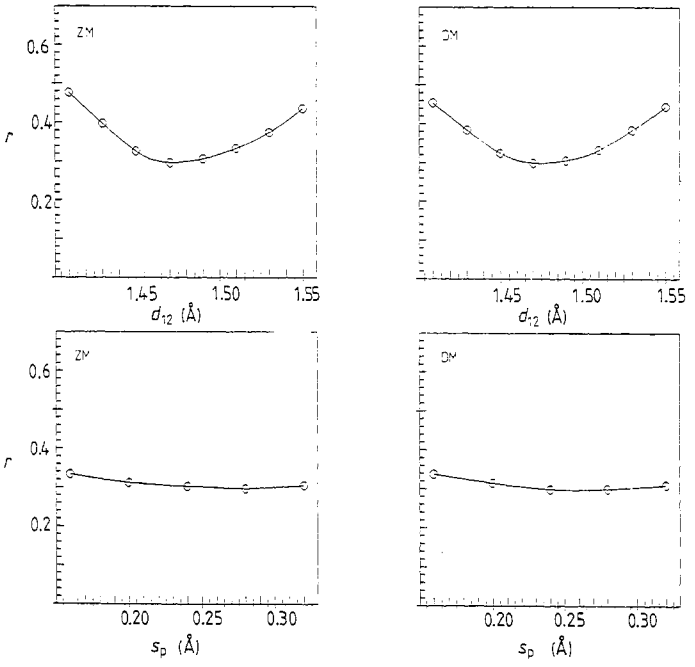

Figure 7. *r*-factors for the ZM (figure 1(*a*)) and DM (figure 1(*d*)) as a function of d_{12} and s_p at off-normal incidence ($\vartheta = 14°$, $\varphi = 146°$).

sensitive beams was too small. So no clear discrimination between the ZM and DM can be made using the present off-normal incidence data. Nevertheless, the structural parameters obtained agree with those resulting from the normal incidence analysis. This is demonstrated in figure 7, which displays the r-factor minima at $s_p = 0.28$ Å and at $s_p = 0.26$ Å for the ZM and DM respectively.

5. Discussion and conclusion

As described, numerous model calculations were tried in this work to enable us to solve the c(2 × 2) W(100) reconstruction. We followed the strategy of using the quasi-dynamical method in a first step and then refining the favourable models by the full dynamical treatment. Clearly we can rule out a surface reconstruction with pure vertical atomic displacements. For models with both parallel and vertical displacements, the latter could be shown to be rather small, i.e. below 0.04 Å.

Therefore, the present analysis strongly favours a reconstruction model with dominant in-plane atomic displacements. We find a minimum Pendry r-factor, $r = 0.26$, as averaged over seven symmetrically non-equivalent beams for the ZM proposed by Debe and King (1977, 1979). This is the best theoretical and experimental agreement reported so far for the W(100) reconstruction. It results from allowing the reconstructive movement of atoms to extend to the second atomic layer, where the in-plane amplitudes are $s_{p1} = 0.24$ Å and $s_{p2} = 0.02$ Å with inter-layer distances $d_{12} = 1.47$ Å and $d_{23} = 1.60$ Å (bulk value $d_0 = 1.58$ Å). This is in agreement with earlier LEED analyses, considering, however, only first-layer atomic shifts and yielding a less satisfactory theoretical and experimental fit. There is also quantitative agreement with a recent investigation using x-rays (Robinson *et al* 1987). Moreover, there is agreement with theoretical predictions for the decay of atomic displacements in layers of increasing depth (Fasolino and Tosatti 1987). However, due to the normal or near-normal incidence for which our data were recorded, the uncertainty for the in-plane displacements is rather high, i.e. $\Delta s_{p1} = \pm 0.11$ Å and $\Delta s_{p2} = \pm 0.02$ Å, while that for inter-layer distances is as low as usual (±0.03 Å). Moreover, this restricted sensitivity with respect to parallel atomic shifts does not allow us to rule out clearly other models of in-plane displacements. So we find an only slightly increased r-factor ($r = 0.28$) for the DM, although the fit could possibly be further improved by allowing the reconstruction to extend to the second layer as in the case of the ZM. It is the authors' view that only data taken at a very oblique incidence would allow us to discriminate between the various models of in-plane reconstruction.

Acknowledgment

The authors gratefully acknowledge the financial support of the Deutsche Forschungsgemeinschaft (DFG).

References

Barker R A, Estrup P J, Jona F and Marcus P M 1978 *Solid State Commun.* **25** 375–9

Bickel N and Heinz K 1985 *Surf. Sci.* **163** 435–43

Bickel N, Heinz K, Landskron H, Rous P J, Pendry J B and Saldin D K 1987 *Proc. 2nd Int. Conf. Structure of Surfaces* (Berlin: Springer) pp 19–25

Debe M K and King D A 1977 *Phys. Rev. Lett.* **39** 708–11
—— 1979 *Surf. Sci.* **81** 193–237
Fasolino A and Tosatti E 1987 *Phys. Rev.* B **35** 4264–83
Felter T E, Barker R A and Estrup P J 1977 *Phys. Rev. Lett.* **38** 1138–41
Heilmann P, Heinz K and Müller K 1979 *Surf. Sci.* **89** 84–94
Heilmann P, Lang E, Heinz K and Müller K 1985 *Determination of Surface Structure by* LEED (New York: Plenum) pp 463–81
Heinz K and Besold G 1983 *Surf. Sci.* **125** 515–29
Heinz K and Müller K 1982 *Springer Tracts in Modern Physics* vol 91 (Berlin: Springer) pp 1–53
Pendry J B 1974 *Low Energy Electron Diffraction* (London: Academic)
—— 1980 *J. Phys. C: Solid State Phys.* **13** 937–44
Robinson I K, Altmann M S and Estrup P J 1987 *Proc. 2nd Int. Conf. Structure of Surfaces* (Berlin: Springer) pp 137–41
Stensgaard I, Feldman L C and Silverman P J 1979 *Phys. Rev. Lett.* **42** 247–50
Tung T, Graham R and Melmed A J 1982 *Surf. Sci.* **115** 576–98
Van Hove M A and Tong S Y 1979 *Surface Crystallography by* LEED (Berlin: Springer)
Van Hove M A, Weinberg W H and Chan C-M 1986 *Low-Energy Electron Diffraction* (Berlin: Springer)
Walker J A, Debe M K and King D A 1981 *Surf. Sci.* **104** 405–18
Wang G-C and Lu T-M 1982 *Surf. Sci.* **122** L635–41
Wendelken J F and Wang G-C 1985 *Phys. Rev.* B **32** 7542–4
Yonehara K and Schmidt L D 1971 *Surf. Sci.* **25** 238–60